LETTER

https://doi.org/10.1038/s41586-018-0371-0

Extensive loss of past permafrost carbon but a net accumulation into present-day soils

Amelie Lindgren[1,2]*, Gustaf Hugelius[1,2] & Peter Kuhry[1,2]

Atmospheric concentrations of carbon dioxide increased between the Last Glacial Maximum (LGM, around 21,000 years ago) and the preindustrial era[1]. It is thought that the evolution of this atmospheric carbon dioxide (and that of atmospheric methane) during the glacial-to-interglacial transition was influenced by organic carbon that was stored in permafrost during the LGM and then underwent decomposition and release following thaw[2,3]. It has also been suggested that the rather erratic atmospheric $\delta^{13}C$ and $\Delta^{14}C$ signals seen during deglaciation[1,4] could partly be explained by the presence of a large terrestrial inert LGM carbon stock, despite the biosphere being less productive (and therefore storing less carbon)[5,6]. Here we present an empirically derived estimate of the carbon stored in permafrost during the LGM by reconstructing the extent and carbon content of LGM biomes, peatland regions and deep sedimentary deposits. We find that the total estimated soil carbon stock for the LGM northern permafrost region is smaller than the estimated present-day storage (in both permafrost and non-permafrost soils) for the same region. A substantial decrease in the permafrost area from the LGM to the present day has been accompanied by a roughly 400-petagram increase in the total soil carbon stock. This increase in soil carbon suggests that permafrost carbon has made no net contribution to the atmospheric carbon pool since the LGM. However, our results also indicate potential postglacial reductions in the portion of the carbon stock that is trapped in permafrost, of around 1,000 petagrams, supporting earlier studies[7]. We further find that carbon has shifted from being primarily stored in permafrost mineral soils and loess deposits during the LGM, to being roughly equally divided between peatlands, mineral soils and permafrost loess deposits today.

It has been proposed previously that the global terrestrial carbon stock increased from the LGM to the present day[8,9]. However, these studies did not explicitly consider permafrost or deep-soil carbon stocks, which would have caused them to underestimate soil carbon storage in certain regions during the LGM. Moreover, these studies did not look at the potential loss of permafrost-trapped soil carbon during deglaciation—information that is needed to resolve atmospheric isotope signals[2]. Modern permafrost soils store considerable amounts of organic carbon[10]; because of this, it has been suggested that the larger area of permafrost during the LGM area[11] and the greater extent of permafrost loess deposits[6] led to higher-than-present soil carbon storage at that time. In the absence of empirical reconstructions of carbon storage within the LGM permafrost zone, estimates have relied on model outputs and endmember calculations[5,12]. However, present Earth system models (ESMs) cannot represent the key processes of glacial-to-interglacial CO_2 dynamics owing to uncertain parameterization of peat and permafrost carbon dynamics[13]. Although ESMs are improving rapidly[12,14] and hold the potential of projecting forwards in time, they must still rely on empirical palaeontological data for validation of past glacial cycles.

Here we combine an extensive range of empirical data on past environments to explore and categorize the LGM permafrost landscape, and to compare it with the present-day landscape in the same region. We define carbon stored in permafrost itself as inert, and compare how this inert fraction of the total carbon stock changed from the LGM to the present.

As the basis of our calculations, we adapted LGM biome reconstructions[15–17] to delineate areas that were dominated by tundra, forest and steppe biomes, all of which encompassed a variety of plant communities (Fig. 1a and Extended Data Table 1). Within these broader categories, we differentiated lowland and alpine zones[18], as well as zones with lower or higher peatland coverage (Fig. 1b) according to findings of buried peat and counts of *Sphagnum* moss spores in pollen assemblages (Extended Data Fig. 1). To reconstruct typical carbon stocks for these past regions, we compared them with modern-day tundra, taiga and steppe within the present permafrost zone[19]. By assuming a comparable magnitude and variability of landscape carbon stocks between past and present biomes, we estimated LGM carbon stocks down to a depth of 3 metres on the basis of present-day data from North America[20] for taiga and tundra, and from the Tibetan plateau[21] for steppe (Extended Data Table 2). Alpine regions with steep mountain slopes were reconstructed separately. We calculated a mineral-soil carbon stock of 790 Pg for the whole LGM permafrost region, mainly from carbon-rich tundra soils (Table 1). A striking difference between past and modern permafrost environments is the apparent lack of peatlands at LGM times. Extensive databases and previous research notwithstanding, records of northern peatlands older than 16.5 thousand years are scarce[22], indicating limited peatland development during LGM times. Consequently, we reconstructed an LGM peatland carbon stock of only 30 Pg.

Because sea levels during the LGM were lower than today, the LGM landscape included areas of exposed sea shelves. We included 0–3 metres' depth of carbon stocks from these areas in our overall biome reconstructions, amounting to an additional carbon storage of 220 Pg. We assume that these shelves, which have since been inundated by the sea, have retained the carbon accumulated during glacial times. Very limited data are available for sea-shelf carbon stocks[23], but we assume that any carbon that may have been lost through sub-sea permafrost degradation and microbial decomposition has been compensated by fresh sediment deposition. Another important landscape element during glacial times was the ice sheets themselves. Preglacial landscapes might have been partially preserved under these cold-based sheets[24] (Extended Data Fig. 2), and we reconstructed an inert LGM carbon stock of 120 Pg from these subglacial areas. We assume no changes to carbon stocks beneath the still-existent Greenland Ice Sheet (50 Pg).

Extensive areas with loess sequences in the Northern Hemisphere formed over several glacial periods, including the LGM, and it has been proposed that their accumulative genesis resulted in carbon-rich deposits across the past permafrost zone[6], similar to the Beringian Yedoma deposits (Fig. 1b; Yedoma deposits are organic- and ice-rich permafrost of Pleistocene age). The depth and carbon stocks of these deposits are included in our LGM carbon estimate. However, we conclude that deposits pre-dating the coldest interval of the last glacial period (marine isotope stages 4–2)—which lie outside the present northern permafrost region—were affected by (repeated) thaw in warm

[1]Department of Physical Geography, Stockholm University, Stockholm, Sweden. [2]Bolin Centre for Climate Research, Stockholm University, Stockholm, Sweden. *e-mail: amelie.lindgren@natgeo.su.se

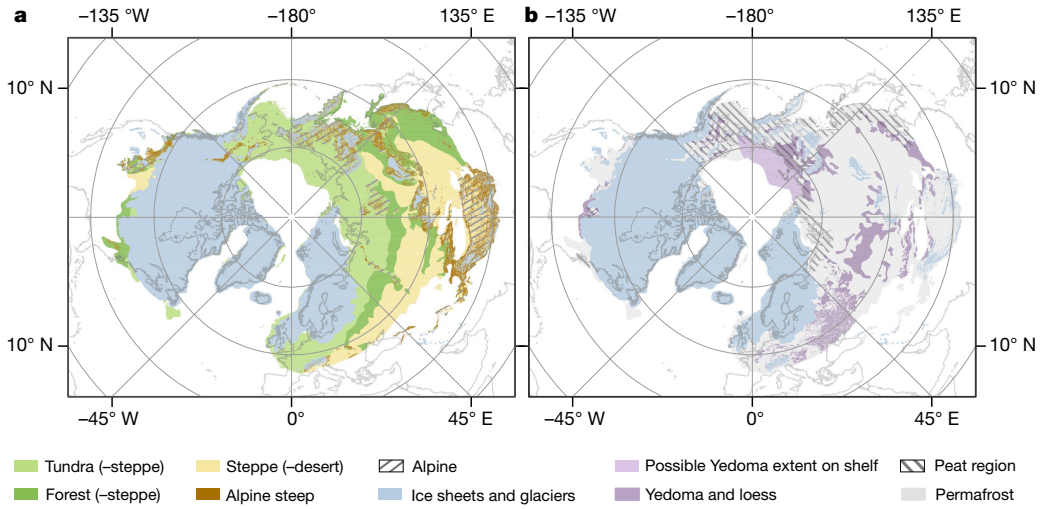

Fig. 1 | Reconstructed LGM environment. a, 'Mega' biomes (defined in Extended Data Table 1) and ice-sheet extents in the LGM northern permafrost region. In parentheses are assumed secondary occurrences of other biome types within broader mega biomes. **b**, Spatial extents of permafrost, Yedoma, loess and peat regions in the LGM northern permafrost region. The Yedoma and loess deposits include the majority of our deep deposits, with additional carbon storage occurring in deltas (extent not reconstructed). The peat region depicts areas in which we reconstruct a higher LGM peat coverage of 5%, compared with 1% in other regions (that is, areas within the LGM permafrost region but outside of the peat region).

interglacial and interstadial periods before the LGM. This resulted in a substantial depletion of their initial high carbon stocks before the LGM, and we reconstructed an additional storage of 366 Pg carbon (range 56–725 Pg) during the LGM, which is far less than the 1,000 Pg suggested previously[6]. We assumed that other deep permafrost carbon stocks—such as those on the Siberian shelf, in deltas, and in the current Yedoma region (Table 1) —were constant between the LGM and the present, with small changes in the inert component. We have not explicitly considered stocks in other deep Quaternary deposits[8], but assume that they have remained constant.

Surprisingly, we find that the total estimated soil carbon stock for the LGM northern permafrost region is smaller than the estimated present-day storage (in both permafrost and non-permafrost soils), if the same areas are compared (2,300 Pg and 2,700 Pg, respectively; Table 1 and Supplementary Table 4). We assessed uncertainties in our reconstructions and determined a plausible maximum and minimum range of LGM permafrost carbon stocks of between 1,680 Pg to 2,860 Pg (Table 1; present-day range 2,440–3,070 Pg). We used a range of scenarios for uncertainty quantification because the nature of this LGM reconstruction precludes traditional statistical quantification of variance or uncertainty. These error ranges represent the main reconstruction uncertainties—that is, the average carbon density of different LGM ecosystems, the distribution of biomes, the areal coverage of peatlands, storage in deep loess deposits and the possible storage of carbon beneath ice sheets. We provide a longer discussion about uncertainties in the Supplementary Information.

The net gain of carbon from 2,300 Pg in the LGM to 2,700 Pg at present does not imply gradual carbon accumulation following postglacial warming and permafrost thaw. Instead, from LGM times to the present there is evidence for a geographic shift in carbon storage. There has been a net transfer of carbon from mineral permafrost soils and subglacial and deep deposits, via the atmosphere, into thawed mineral soil and both frozen and thawed organic soils (Fig. 2). Previous empirical studies have also noted an increase in global terrestrial carbon storage, including in vegetation, over the same period[8]. Carbon storage in both vegetation and soils may also have been higher

Table 1 | Estimated carbon pools (in Pg C) for the LGM and present day

	LGM	Range	LGM inert	Range	Present	Range	Present inert	Range
Mineral soil (0–3 m)	790	269–1143	574	177–838	1084	840–1,366		
(of which permafrost region)					(589)	367–811	439	270–608
Peatland (0–3 m)	30	16–180	20	11–121	550	457–683		
(of which permafrost region)					(153)	91–215	127	75–179
Shelf (0–3 m)	220	64–252	164	41–183	220	64–251		
(of which permafrost region)					(122)	33–130		
Deep deposits: Yedoma (>3 m)	741	610–884	741	610–884	741	624–869		
(of which permafrost region)					(718)	601–846	669	564–785
Deep deposits (>3 m): loess	366	56–725	366	56–725	48	9–92		
Deltas	91	37–135	91	37–135	91	37–135	69	31–107
Large lakes	2				45			
Subglacial	170	117–225	171	117–225	(48)		48	
Total	**2,319**	**1,677–2,867**	**2,035**	**1,456–2,522**	**2,736**	**2,436–3,073**	**1,283**	**1,077–1,495**

This table summarizes and compares carbon storage during the LGM and present-day carbon storage within the same region, including the permafrost-inert part of each stock. Woody litter is not included. Deep deposits are separated into Yedoma and loess, where the former includes Yedoma carbon storage on sea shelves. Plausible range scenarios for the upper three metres of soil are estimated for the LGM (see Methods). The range for the deep deposits includes both well constrained error estimates from present deposits and a statistical analysis of the depth distribution for additional LGM permafrost loess deposits. The total ranges were calculated by additive error propagation. For more details and descriptions of how the present-day C pool was quantified, see Methods, Supplementary Information and Supplementary Table 4.

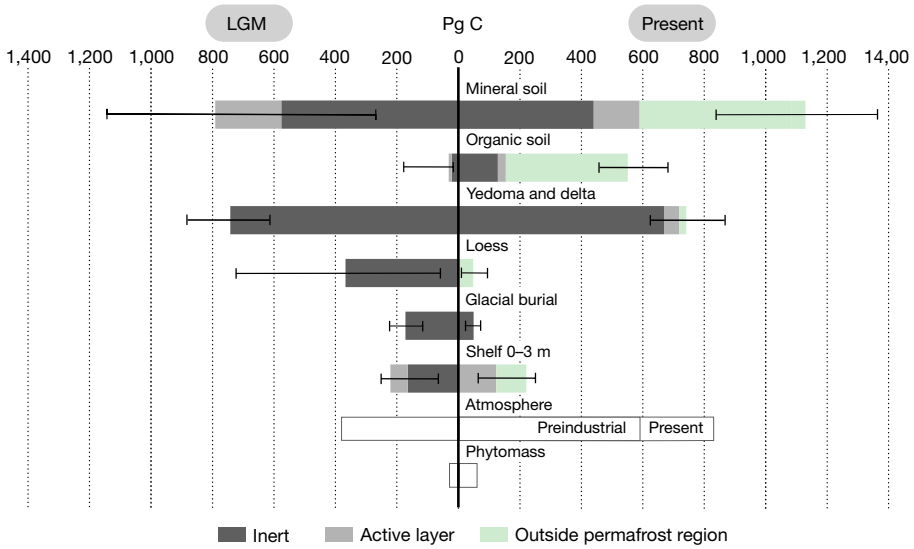

Fig. 2 | Sizes of carbon stocks in the LGM northern permafrost region during the LGM and at present. Separate stocks are reported for total carbon (shown by the total length of each bar), separated into inert carbon (dark grey; defined as permanently frozen carbon), active-layer carbon (light grey; defined as carbon within the seasonally thawed layer of soil above the permafrost table), and unfrozen carbon outside the modern permafrost region (light green). Carbon stocks in the atmosphere and in plant material (phytomass) from the LGM northern permafrost region are included in the figure for reference, but are not included in the total carbon stocks discussed in the text. The carbon stocks of large lakes are not shown separately, but are included in the mineral-soil carbon as unfrozen (not visible for the LGM). Error bars are ranges around the total carbon stocks, specified in Table 1 and Methods.

than at present at some point during the Holocene epoch[8,9]. Our estimate of the LGM inert permafrost carbon stock (2,000 Pg carbon) is somewhat lower than suggested previously[5,12] (2,300 Pg), but is much larger than the present inert permafrost carbon stock (1,300 Pg). This agrees with previous findings of postglacial permafrost carbon remobilization[3]. known thermokarst events (ground subsidence caused by the melting of massive ground ice) in the current Yedoma region postdate the LGM[3], and our review of loess sequences located outside the present-day permafrost region shows no evidence of thermokarst at LGM times. The thaw of permafrost deposits following postglacial warming would have exposed organic matter to decomposition, resulting in the release of carbon depleted relative to the atmosphere in both $\Delta^{14}C$ (on account of its greater age) and $\delta^{13}C$ (caused by the preference of light-carbon uptake by plants and further fractionation during decomposition). These isotopic properties of the thawed material fit well with the development of atmospheric isotopic signals preserved in ice cores[1,4]. Decomposition of a putative, but highly uncertain, old and inert subglacial carbon stock following the gradual retreat of the large Northern Hemisphere ice sheets could also have contributed to these observed changes in atmospheric isotope composition.

While widespread thermokarst formation occurred in the Yedoma region during the Late Glacial and Early Holocene[3], new land areas became available for soil development following deglaciation of the Laurentide and Fennoscandian ice sheets[25]. This also corresponds to a time period of widespread peatland formation in the Northern Hemisphere[22]. The postglacial environment has changed dramatically, and parts of the landscape that were previously occupied by the relatively dry tundra (or tundra–steppe) are today covered by peat soils[26]. These organic soils represent a considerable portion of the present Northern Hemisphere carbon stocks[27]. Therefore, the glacial–interglacial transition seems to correspond to a period involving a depletion of permafrost carbon stocks, while at the same time new stocks started to accumulate in other soils[25]. In the present discontinuous permafrost region, the aggradation of new permafrost into previously accumulated peat deposits following Late Holocene cooling has resulted in the formation of new inert carbon storage. Considering all of these lines of evidence, it is possible that around 1,000 Pg of inert carbon became activated during the deglaciation.

By their nature, reconstructions of past ecosystems and environments rely on assumptions that are highly uncertain and difficult to validate. Through the use of analogous modern-day landscapes, we assume a comparable magnitude and variability of soil carbon stocks between past and present. However, LGM plant communities existed in forms we do not see today, such as the steppe–tundra biome with its co-dominance of steppe and tundra plant species[28]. Plant productivity, and carbon input to soils, was probably lower owing to lower atmospheric CO_2 concentrations. This may have been especially important in forest systems, as low CO_2 levels favoured more open vegetation[9], but the response of cold-region ecosystems to variable ambient CO_2 levels remains uncertain even today, and experiments show that changes in plant productivity under different CO_2 concentrations do not necessarily change ecosystem carbon storage[29]. Some authors have suggested that fast biochemical cycling because of the presence of large grazers (Extended Data Fig. 3), and elevated dust loads supplying fresh nutrients, enabled productive, and carbon-rich, ecosystems during the LGM[6,30]. This idea is supported by the high carbon stocks observed in the preserved LGM Yedoma region, similar to those we reconstruct, but it is unclear to what extent the preserved Yedoma is representative of the vast LGM region.

The extent of peatlands and wetlands during the LGM is also highly uncertain. Our reconstructions are based partly on the occurrence of *Sphagnum* spores, but this could have led us to miss minerotrophic fens characterized by graminoids and brown mosses. The scenario-based analysis also shows a skewed error range towards a possibly higher carbon storage. On the other hand, few deep peat deposits are dated to LGM times. Most of the stratigraphic evidence points towards thin (less than 40 cm) peat layers, which in our reconstructions are included in upland mineral-soil reconstructions. Speculation regarding a possible widespread oxidation of LGM peat deposits before the onset of postglacial peatland development lies outside the scope of this empirically based study.

To alleviate some of these uncertainties and to further refine estimates of glacial to interglacial carbon-stock dynamics, further research is needed. Specifically, we propose further research into potential subglacial carbon storage, the initial stock and fate of carbon on inundated sea shelves, the potential extent of peatlands and wetlands during the LGM, and the effect of both lower and higher

atmospheric CO_2 levels on tundra and boreal forest productivity and carbon turnover.

Our reconstructions suggest that the loss of more than 10 million square kilometres of northern permafrost area since the LGM has resulted in the net addition of several hundred petagrams of carbon into present-day soils. Nevertheless, postglacial warming and permafrost thaw resulted in an initial large loss of inert carbon, which may have approached 1,000 Pg. This initial loss of carbon was compensated by carbon accumulation in permafrost-free mineral soils, in deglaciated terrain, and in peatlands. More research is needed to disentangle transient changes during the early stages of the last deglaciation and postglacial warming. We stress that the response of the LGM permafrost carbon stock to thaw may not be a good analogue for the fate of the present permafrost stock, which has a different composition to that of the past.

Online content

Any Methods, including any statements of data availability and Nature Research reporting summaries, along with any additional references and Source Data files, are available in the online version of the paper at https://doi.org/10.1038/s41586-018-0371-0.

Received: 30 August 2017; Accepted: 14 May 2018;

1. Schmitt, J. et al. Carbon isotope constraints on the deglacial CO_2 rise from ice cores. *Science* **336**, 711–714 (2012).
2. Crichton, K. A., Bouttes, N., Roche, D. M., Chappellaz, J. & Krinner, G. Permafrost carbon as a missing link to explain CO_2 changes during the last deglaciation. *Nat. Geosci.* **9**, 683–686 (2016); corrigendum 9, 795 (2016).
3. Walter, K. M., Edwards, M. E., Grosse, G., Zimov, S. A. & Chapin, F. S. III. Thermokarst lakes as a source of atmospheric CH_4 during the last deglaciation. *Science* **318**, 633–636 (2007).
4. Broecker, W. & Barker, S. A. 190‰ drop in atmosphere's $\Delta^{14}C$ during the 'Mystery Interval' (17.5 to 14.5 kyr). *Earth Planet. Sci. Lett.* **256**, 90–99 (2007).
5. Ciais, P. et al. Large inert carbon pool in the terrestrial biosphere during the Last Glacial Maximum. *Nat. Geosci.* **5**, 74–79 (2011).
6. Zimov, N. S. et al. Carbon storage in permafrost and soils of the mammoth tundra-steppe biome: Role in the global carbon budget. *Geophys. Res. Lett.* **36**, L02502 (2009).
7. Anthony, K. M. W. et al. A shift of thermokarst lakes from carbon sources to sinks during the Holocene epoch. *Nature* **511**, 452–456 (2014).
8. Adams, J. M., Faure, H., Faure-Denard, L., McGlade, J. M. & Woodward, F. I. Increases in terrestrial carbon storage from the Last Glacial Maximum to the present. *Nature* **348**, 711–714 (1990).
9. Prentice, I. C., Harrison, S. P. & Bartlein, P. J. Global vegetation and terrestrial carbon cycle changes after the last ice age. *New Phytol.* **189**, 988–998 (2011).
10. Hugelius, G. et al. Estimated stocks of circumpolar permafrost carbon with quantified uncertainty ranges and identified data gaps. *Biogeosciences* **11**, 6573–6593 (2014).
11. Lindgren, A., Hugelius, G., Kuhry, P., Christensen, T. R. & Vandenberghe, J. GIS-based maps and area estimates of Northern Hemisphere permafrost extent during the Last Glacial Maximum. *Permafr. Periglac. Process.* **27**, 6–16 (2016).
12. Zhu, D. et al. Simulating soil organic carbon in yedoma deposits during the Last Glacial Maximum in a land surface model. *Geophys. Res. Lett.* **43**, 5133–5142 (2016).
13. Brovkin, V. et al. Comparative carbon cycle dynamics of the present and last interglacial. *Quat. Sci. Rev.* **137**, 15–32 (2016).
14. Kleinen, T., Brovkin, V. & Munhoven, G. Modelled interglacial carbon cycle dynamics during the Holocene, the Eemian and Marine Isotope Stage (MIS) 11. *Clim. Past* **12**, 2145–2160 (2016).
15. Grichuk, V. P. in *Late Quaternary Environments of the Soviet Union* (ed. Velichko, A. A.) 155–178 (Longman, 1984).
16. Dyke, A. S. Late Quaternary vegetation history of northern North America based on pollen, macrofossil, and faunal remains. *Geogr. Phys. Quat.* **59**, 211–262 (2005).
17. Baryshnikov, G. A. & Markova, A. K. in *Paleoclimates and Paleoenvironments of Extra-tropical Regions of the Northern Hemisphere. Late Pleistocene–Holocene. Atlas-monograph* (ed. Velichko, A. A.) 79–87 (GEOS, 2009).
18. Gruber, S. Derivation and analysis of a high-resolution estimate of global permafrost zonation. *Cryosphere* **6**, 221–233 (2012).
19. Olson, D. M. et al. Terrestrial ecoregions of the world: a new map of life on Earth. *Bioscience* **51**, 933–938 (2001).
20. Hugelius, G. et al. The northern circumpolar soil carbon database: spatially distributed datasets of soil coverage and soil carbon storage in the northern permafrost regions. *Earth Syst. Sci. Data* **5**, 3–13 (2013).
21. Ding, J. et al. The permafrost carbon inventory on the Tibetan Plateau: a new evaluation using deep sediment cores. *Glob. Change Biol.* **22**, 2688–2701 (2016).
22. Macdonald, G. M. et al. Rapid early development of circumarctic peatlands and atmospheric CH4 and CO2 variations. *Science* **314**, 285–288 (2006).
23. Schuur, E. A. G. et al. Climate change and the permafrost carbon feedback. *Nature* **520**, 171–179 (2015).
24. Kleman, J. & Hattestrand, C. Frozen-bed Fennoscandian and Laurentide ice sheets during the Last Glacial Maximum. *Nature* **402**, 63–66 (1999).
25. Harden, J. W., Sundquist, E. T., Stallard, R. F. & Mark, R. K. Dynamics of soil carbon during deglaciation of the Laurentide Ice Sheet. *Science* **258**, 1921–1924 (1992).
26. Loisel, J. et al. Insights and issues with estimating northern peatland carbon stocks and fluxes since the Last Glacial Maximum. *Earth Sci. Rev.* **165**, 59–80 (2017).
27. Yu, Z. C. Northern peatland carbon stocks and dynamics: a review. *Biogeosciences* **9**, 4071–4085 (2012).
28. Willerslev, E. et al. Fifty thousand years of Arctic vegetation and megafaunal diet. *Nature* **506**, 47–51 (2014).
29. Norby, R. J. & Zak, D. R. Ecological lessons from free-air CO_2 enrichment (FACE) experiments. *Annu. Rev. Ecol. Evol. Syst.* **42**, 181–203 (2011).
30. Yurtsev, B. A. The Pleistocene 'tundra-steppe' and the productivity paradox: the landscape approach. *Quat. Sci. Rev.* **20**, 165–174 (2001).

Acknowledgements This study was funded by a French–Swedish cooperation grant from the Swedish Research Council (349-2012-6293), and by the European Union (EU) Joint Programming Initiative (JPI) Climate Constraining Uncertainties in the Permafrost–Climate Feedback (COUP) consortium. G.H. acknowledges a Marie Curie Skłodowska and Swedish Research Council International Career Grant (INCA; no. 330-2014-6417). We also acknowledge J.-O. Persson at the Department of Mathematics, Stockholm University, who assisted with statistical consulting, and the Bolin Centre for Climate Research for hosting the data.

Reviewer information *Nature* thanks V. Brovkin, N. Pastick and the other anonymous reviewer(s) for their contribution to the peer review of this work.

Author contributions A.L. was responsible for data collection, digitization of data, and analysis of data from past environments, excluding deep loess deposits. P.K. was responsible for the review and analysis of deep loess deposits. G.H. was responsible for estimates of modern carbon pools. All authors contributed substantially to formulating the research idea, interpreting the results and writing the paper.

Competing interests The authors declare no competing interests.

Additional information
Extended data is available for this paper at https://doi.org/10.1038/s41586-018-0371-0.
Supplementary information is available for this paper at https://doi.org/10.1038/s41586-018-0371-0.
Reprints and permissions information is available at http://www.nature.com/reprints.
Correspondence and requests for materials should be addressed to A.L.
Publisher's note: Springer Nature remains neutral with regard to jurisdictional claims in published maps and institutional affiliations.

METHODS

Biome reconstructions. Empirical map reconstructions of LGM biomes—based on pollen, plant macrofossils and/or faunal remains[15–17]—were reviewed, digitized and compared to produce an aggregate biome-reconstruction map for the LGM permafrost region. The individual classes were harmonized to a common and simplified biome classification scheme (Extended Data Table 1). This harmonization required us to generalize biomes into the following broader categories: tundra (–steppe), forest (–steppe), and steppe (–desert), where each category in parenthesis defines secondary vegetation types. Findings of LGM megafaunal remains[17,31,32] were briefly reviewed as a complement to the biome reconstructions (see Supplementary Information and Extended Data Fig. 3). The resulting map was compared with independent data points of biomized pollen counts[9,33–36] (Kappa 0.85; see Supplementary Information and Extended Data Fig. 4).

Following the same overall procedure, we harmonized reconstructions of various alpine environments into alpine mega biomes (Extended Data Table 1). Moreover, using present-day topographic data (we assume no major changes in topography since the LGM), we categorized additional areas as alpine if they display a ruggedness index equal to or larger than 4. For more information about the procedure and data used for this classification, see ref. [18]. By categorizing areas as rugged, a reconstructed tundra (–steppe) area becomes alpine tundra (–steppe), and so on. This scheme also allows mountain ranges such as the Alps to be identified as alpine.

Steep areas in cold climates are characterized by thin soils, talus formations and limited vegetation coverage, while valley floors may accumulate more carbon-rich soils (see, for example, ref. [37]). On the basis of terrain slope[38] for the (mixed) alpine and topographically rugged areas, we separated steep areas from valley floors with a slope threshold of 4 degrees[39] (see Supplementary Information for details).

Peatlands. We digitized a reconstructed possible LGM peatland region on the basis of a range of evidence indicative of the presence of peatland (Extended Data Fig. 1). This included previous reconstructions of LGM peatlands[40,41], local to regional studies of peat[42,43] and peaty (with O-horizons between 10 cm and 40 cm thick) deposits[44–49], and palynological data of *Sphagnum* spores[34,50–64]. The delineation of the possible peatland regions was done by hand, including previously reported regions, and generally accepting *Sphagnum* spore counts greater than 1% (ref. [40]) with indicative age control. Spore percentages below 1% were not accounted for unless they occurred in relatively close proximity. We do not take ruggedness into account when estimating the extent of this region. Further methods are available in the Supplementary Information.

To estimate peatland extent within the 'possible peatland region', we hypothesized that continental and dry climates are less favourable to peat formation, so that present circumarctic peatland extent is related to continentality. We supported this hypothesis by comparing a map[65] of the Gorczynski continentality index[66] (K_G), based on Climatic Research Unit (CRU) climate data from 1951 to 2000, with maps of peatland extent in flat terrain (ruggedness less than 2) within the current permafrost regions of North America and Eurasia[20] ($R^2 = 0.40$; $P = 0.07$; Extended Data Fig. 5). We thus assume that the modern peatland extent is a reasonable analogue of LGM conditions. With a dry, cold climate during the LGM[67,68], similar to conditions in highly continental areas today, we reconstruct peatland coverage in the 'possible peatland regions' as around 5%, which is the average coverage in the most continental region in Siberia[20]. In addition, peaty soils may have been present across larger areas, but these are included in the mineral-soil transfer functions from modern analogues to the LGM (see Extended Data Table 2). We assigned areas outside the peatland region a peatland coverage of 1%, so as to not entirely discount peatland presence in localized settings.

Soil carbon-transfer functions. To calculate LGM soil carbon for the different biome and landscape types, we relied on modern-day analogues and the carbon storage in these systems. For the tundra (–steppe) and forest (–steppe) mega biomes, we constructed carbon-transfer functions by extracting soil carbon data from the North American continent presented in the NCSCDv2 database[20], which we subdivided into tundra, alpine tundra, taiga and alpine taiga biomes. The biome subdivision was based on the Terrestrial Ecoregions of the World data set[19]. Using the permafrost map of ref. [69], we also categorized these data according to continuous or discontinuous permafrost (including all non-continuous permafrost zones in the discontinuous category).

We decided to use only North American data to calculate our carbon-transfer functions because the spatial soil carbon scaling in this region is explicitly linked to different soil series (US) or soil names (Canada). For other regions, the NCSCDv2 database was created on the basis of more generalized scaling. Where NCSCDv2 is scaled at the soil-series/soil-names level, it has a more realistic representation of landscape scale variability. This in turn translates into a more realistic estimate of scaling errors. There was a concern that simplified thematic scaling, as applied in other NCSCDv2 regions, could cause underestimation of actual variability and associated scaling errors.

For each category, we calculated averages of kg C m^{-2} (transfer functions) normalized by polygon area for each separate category, as follows:

$$\overline{C} = \frac{\sum_{i=1}^{n} C_i}{\sum_{i=1}^{n} a_i}$$

where $\overline{C}$ is the weighted average kg C m^{-2} (transfer function), C_i is the mineral carbon content of each polygon belonging to that category (excluding histosols and histels), and a_i is the mineral-soils area for each polygon.

We used relationships of soil carbon with depth for the 1–3-m interval according to an analysis of soil profiles[70], from which we estimate carbon content at depth as a simple function of carbon content at 0–1 m. As an example, in tundra (–steppe) on continuous permafrost, the carbon content at 2 m depth was 48% of the carbon content at 1 m. For each separate transfer function, we calculated the following:

$$\overline{C}_2 = f(\overline{C}_1)$$
$$\overline{C}_3 = f(\overline{C}_1)$$

Where $\overline{C}_2$ is the weighted average C m^{-2} at 2 m depth, and $\overline{C}_3$ is for 3 m. Detailed results are given in Extended Data Table 2, with a quick overview in Extended Data Fig. 6.

We estimated transfer functions for steppe (–desert) by using modern-day data from the Qinghai–Tibetan Plateau[21]. The overall means for moist and dry Qinghai–Tibetan Plateau permafrost grasslands were used as analogues for all LGM steppe biomes. Data for the transfer functions for 0–1 m, 1–2 m and 2–3 m were extracted from Fig. 4 and the supplement of ref. [21] Data for 0–30 cm depth were interpolated from a linear regression of log(depth) to log(soil C) ($R^2 > 0.99$; $P < 0.05$).

Steep areas in alpine and mixed alpine regions with a slope of more than 4 degrees were treated separately and given a default value of 3 kg C m^{-2} on the basis of ref. [37].

The carbon-transfer functions for peat soils were based on the North American data within NCSCDv2, across all categories regardless of biome, but with distinctions between continuous and discontinuous permafrost as well as between lowland and alpine conditions. These carbon-transfer functions were applied down to 1 m only, because of limited evidence for deeper peat deposits at LGM times. With a few exceptions[42,43], most records of LGM peat refer to thin peat layers[44–49]. Therefore, a carbon-transfer function considering 1 m of peat might still be an overestimate. For 1 m to 3 m, we applied the mineral-soil carbon-transfer functions that corresponded to the assigned biome for that area.

Modern-day soil carbon estimates. The LGM permafrost region extends over the present-day northern permafrost region and over large areas that are presently permafrost free. Modern-day soil carbon stocks for the present northern permafrost region were derived from NCSCDv2[20] and from data for the Qinghai–Tibetan Plateau[21]. For areas outside the permafrost region, present-day soil carbon stocks were computed and extracted from the global-scale WISE30sec database[71]. This database contains data for the top 2 m of soil. Soil carbon stocks in the 2–3-m depth interval were extrapolated on the basis of biome-specific ratios of soil carbon in the 1–2-m depth interval to the 2–3-m depth interval from Table 3 of ref. [72]. The spatial scaling of these ratios was applied using spatial biome delineations from ref. [19]. Ref. [72] presents a depth distribution for mineral-soil types only. For peatlands (Histosols), soil carbon in the 2–3-m depth range was estimated to be half of the soil carbon content mapped at the 1–2 m. This scaling is consistent with an overall mean peat depth of 2.3 m (ref. [73]) and assumptions of a typical mineral-soil carbon content below that. We calculated the uncertainty ranges for these soil carbon estimates by using standard formulas of additive error propagation, combining the uncertainty ranges of the 0–2-m carbon stocks[71] with the uncertainty ranges of the extrapolation ratios[72]. Modern carbon stocks are detailed in Supplementary Table 4.

Lakes. We estimated organic carbon storage in the sediments of large lakes (bigger than 10 km^2) of the northern permafrost region during LGM times and the corresponding area at present[74], using limited available geochemical data (measured/inferred dry bulk density and organic carbon content) and weighing carbon densities by lake size and their sediment depths. The LGM lake extent was based on lakes reconstructed for LGM times[75]. We estimated carbon storage for large lakes only because the databases used to calculate average soil carbon stocks (NCSCDv2 and WISE30sec) do not spatially resolve small lakes. Therefore they are already included in the soil carbon-transfer functions.

During the LGM, large lakes were limited in extent (occupying around 0.2% of the total LGM permafrost area) and largely restricted to ice-free parts of the Eurasian sector. Storage in sediments from marine isotope stage 4 (MIS4) to the LGM was on average 21 kg C m^{-2} (refs. [76–78]), resulting in a total stock of 2 Pg C. In postglacial times, the area occupied by large lakes increased (to around 1.9% of the total area), particularly in North America following the retreat of the Laurentide

Ice sheet. Storage in post-LGM sediments is on average 43 kg C m^{-2} (refs. [76–80]), to which should be added the storage in MIS4–LGM deposits in the Eurasian sector described above. This results in a total present-day estimate for the large-lake area of 45 Pg C. All of these sediments, during both LGM and present-day times, are considered to be in a thawed state and not to contribute to the inert permafrost carbon stocks. Similar to the calculations for thawed-out loess deposits, we consider that carbon stocks in lake sediments pre-dating the MIS4 stage are not part of the LGM or current active carbon cycles.

Phytomass. We calculated the carbon content of phytomass both during the LGM and at present within the LGM northern permafrost region. These estimates are presented in Fig. 2 for reference to the soil carbon storage. The LGM phytomass (30 Pg C) is based on our biome classification together with phytomass estimates[9]. Present-day above-ground and below-ground biomass in the former LGM permafrost and ice-sheet regions was quantified to 61 Pg C (37 Pg in the LGM permafrost region and 24 Pg in the ice-sheet extent[81]).

Loess reconstruction. We conducted a review of loess and Yedoma studies to calculate the areal extent (Extended Data Fig. 2), average depth and carbon content of those loess sections that lie outside the current permafrost region (Supplementary Table 3). We estimated a total area of additional loess in the LGM northern continuous permafrost region of 2.7 million km^2, mostly in lowland areas. We calculated average depths of these loess deposits across five separate regional sectors (III, Alaska; IV, northern Europe including northwest Russia; V, Siberia; VI, central loess plateau China; and VII, northeast China). To account for differences in the geochemistry and permafrost extent of each sector, we separated the loess into time intervals of origin of 71–45 kyr ago and 45–19 kyr ago. To avoid double accounting, we removed 2 m from the top (roughly corresponding to an original 3 m of sediment if we account for initial excess ground-ice content), because this interval is accounted for in our estimates of soil organic carbon storage for the 0–3-m interval.

To calculate the additional carbon at the time of the LGM, we first conducted an assessment of the present-day carbon content of loess. To infer the carbon densities in these loess deposits at the time of the LGM, we used a survey of published analogues from the present-day Yedoma deposits (Supplementary Tables 2 and 3).

We assume that carbon storage in the current Yedoma region is largely the same as in LGM times (Supplementary Table 3), because the initial carbon losses in Yedoma that resulted from thermokarst following postglacial warming have been compensated by later accumulation in organic-rich lake deposits, peat(y) layers and Holocene soils. Yedoma is also thought to have been prevalent on the Siberian shelf, and therefore we included a deep carbon stock that does not change between past and present. We calculated this carbon stock on the basis of our Yedoma estimates.

A longer and more detailed description of our loess review is available in Supplementary Information.

Glacial burial. We assume that during the LGM, subglacial soil carbon may have been preserved beneath cold-based ice sheets (which are immobile against the ground surface), but that no soil carbon would have been preserved under actively eroding warm-based ice sheets. Following delineations of cold-based ice sheets from ref. [24], we constrained those regions in which we assume that buried permafrost may have been located beneath the Laurentide and Fennoscandian ice sheets[82] (Extended Data Fig. 7). Assuming that, during glaciation, the areas proximal to expanding ice sheets were tundra environments, we applied a transfer function representative of the high arctic tundra (27.5 kg C m^{-2} down to 3 m; ref. [10]) across all areas with cold-based ice-sheets and glaciers. We applied this transfer function both on land and on sea shelves down to 3 m. We assumed that peat covered 1% of the area, but, as previously explained, we did not include any peat deeper than 1 m. Below this peat, we applied mineral-soil carbon estimates down to 3 m. Steep alpine regions were again given a value of 3 kg C m^{-2}. We added an estimate for the Greenland Ice Sheet[69] (1.7 million km^2, 48 Pg C), using the same procedure as described above, although we conclude that the storage beneath the Greenland Ice Sheet has not changed substantially over time.

Shelf areas beneath ice sheets were estimated using a −130 m cut-off[83] on the global relief model ETOPO1 (ref. [84]), meaning that all areas shallower than −130 m were included. This is probably an overestimation, as the sea level reached −130 m only at the very last stages of the glacial period, when the ice sheets were at their largest configuration.

The total storage of carbon beneath cold-based ice, both on land and on sea shelves, amounts to 123 Pg C. However, if we account for the same potential carbon storage beneath warm-based ice sheets as for cold-based ice sheets, the results show an additional 364 Pg C (Extended Data Table 3).

Inert carbon. We define inert carbon as organic carbon in soils or sediments that is protected from potential mineralization by permafrost. Inert carbon would then slowly be depleted in $\Delta^{14}C$, and preserve its isotopic signatures of $\delta^{13}C$ until thaw. Post-thaw microbial processing would also affect the $\delta^{13}C$ of soil organic matter. We categorize all carbon beneath the active layer as inert, and set the active layer to 30 cm depth across all permafrost soils, following ref. [10], and consistent with present-day active-layer depths in tundra on North–Central Siberia[85]. For discontinuous permafrost, we calculate 50% of the area to be inert beneath 30 cm depth, while the remaining area is categorized as entirely active rather than inert. To deal with the potential uncertainty in estimates of the permafrost-inert fraction from the discontinuous permafrost extent and active-layer depths, the reported error ranges of the inert fraction include sensitivity analyses (see below). We assume that all deep carbon stocks, as for those within loess, Yedoma and deltas, were inert during the LGM. Carbon preserved beneath cold-based ice sheets is also inert in this scheme.

For the highly uncertain estimate of carbon on the sea shelves, we consider the 0–3 m stock to have been disturbed during the deglaciation, removing this stock from the inert carbon storage. For the Yedoma on the Siberian shelf, we assume that a portion equivalent to the loss of inert carbon per area from Yedoma on land has become active beneath the sea floor since the LGM. This loss might be underestimated, as wave erosion may have disturbed the Yedoma ice complexes when the sea advanced onto the shelves.

Scenarios and error estimates. Owing to limitations in NCSCDv2, we are unable to use a standard deviation of our carbon-transfer functions for tundra(–steppe) and forest(–steppe) biomes (see Supplementary Information for details). Instead, we calculate and report ranges of potential minimum-to-maximum LGM carbon stocks for the 0–3 m soil. This scheme also deals with area uncertainty within these biome reconstructions. In the first minimum scenario, the tundra (–steppe) and forest (–steppe) categories, both lowland and alpine, were represented by our lowest carbon-transfer function that describes the average carbon content of steppe (–desert). For the steppe (–desert) areas, both lowland and alpine, we calculated a minimum carbon estimate on the basis of the error margins in ref. [21]. For this minimum carbon estimate, we applied a peatland extent of 1% across the LGM permafrost landscape. In the maximum scenario, we applied our highest carbon-transfer function, continuous tundra (–steppe), for those regions that were categorized as lowland or alpine tundra (–steppe) or forest (–steppe). We used the carbon-transfer function for continuous forest (–steppe) to the steppe (–desert) biome so as to not underestimate uncertainty. We also applied a peatland coverage similar to that of today (11%)[20] across the landscape, but with peatland depth limited to 1 m. Steep slopes were not included in these calculations. These scenarios should fully encompass all uncertainties discussed in the Supplementary Information, and are indeed a minimum and a maximum range rather than a range that describes likelihood. We maintain that our best estimate is the most realistic. The error margins for subglacial carbon were calculated by using a ±50% areal coverage of cold-based ice.

Uncertainties in the calculations of the additional LGM permafrost carbon stock in loess deposits are related to area, depth, dry bulk density and per cent carbon estimates. Only for depth have we a nearly complete and consistent data set (see Supplementary Information). We used standard deviations in reported mean depth for all sectors and the two time periods considered (Supplementary Table 3), to obtain a range of 56–725 (366 +359/−310) Pg C for the LGM stocks and 9–92 (48 +44/−39) Pg C for the present remaining stocks in loess deposits.

We conducted an additional sensitivity analysis of the inert carbon by varying the depth of the active layer (30–100 cm) throughout the entire LGM permafrost region and the coverage of permafrost (10–90% coverage) in our LGM discontinuous permafrost zone. This analysis also meant that we estimated additional carbon in loess for the discontinuous zone (51 Pg C) as a maximum scenario (Supplementary Table 4).

All errors or ranges for individual categories (Table 1 and Supplementary Table 4) have been combined by additive error propagation.

Software. We used ArcMap 10.1 in all geographical computations and MS Excel for the final numerical calculations.

Data availability. The biome reconstruction that supports the findings of this study is available at https://bolin.su.se/data/Lindgren-2018, both as a shapefile and in gridded format. Additional sources of used, but unaltered, data sets are referenced within the paper. Compiled data sets are available upon request from the corresponding author.

31. Lorenzen, E. D. et al. Species-specific responses of Late Quaternary megafauna to climate and humans. *Nature* **479**, 359–364 (2011).
32. Nogués-Bravo, D., Rodríguez, J., Hortal, J., Batra, P. & Araújo, M. B. Climate change, humans, and the extinction of the woolly mammoth. *PLoS Biol.* **6**, e79 (2008).
33. Tarasov, P. E. et al. Last glacial maximum biomes reconstructed from pollen and plant macrofossil data from northern Eurasia. *J. Biogeogr.* **27**, 609–620 (2000).
34. Andreev, A. A. et al. Paleoenvironmental changes in Northeastern Siberia during the Late Quaternary—evidence from pollen records of the Bykovsky Peninsula. *Polarforschung* **70**, 13–25 (2000).
35. Andreev, A. A. et al. Vegetation and climate history in the Laptev Sea region (Arctic Siberia) during Late Quaternary inferred from pollen records. *Quat. Sci. Rev.* **30**, 2182–2199 (2011).
36. Ni, J., Cao, X., Jeltsch, F. & Herzschuh, U. Biome distribution over the last 22,000yr in China. *Palaeogeogr. Palaeoclimatol. Palaeoecol.* **409**, 33–47 (2014).

37. Fuchs, M., Kuhry, P. & Hugelius, G. Low below-ground organic carbon storage in a subarctic Alpine permafrost environment. *Cryosphere* **9**, 427–438 (2015).
38. GMTED2010. The Global Multi-resolution Terrain Elevation Data 2010. *US Geological Survey (USGS) Earth Resources Observation & Science (EROS) Center* https://topotools.cr.usgs.gov (2011).
39. Dalrymple, J. B., Blong, R. J. & Conacher, A. J. A hypothetical nine unit landsurface model. *Z. Geomorphol.* **12**, 60–76 (1968).
40. Halsey, L. A., Vitt, D. H. & Gignac, L. D. Sphagnum-dominated peatlands in North America since the Last Glacial Maximum: their occurrence and extent. *Bryologist* **103**, 334–352 (2000).
41. Gajewski, K., Viau, A., Sawada, M., Atkinson, D. & Wilson, S. *Sphagnum* peatland distribution in North America and Eurasia during the past 21,000 years. *Glob. Biogeochem. Cycles* **15**, 297–310 (2001).
42. Baker, R. G., Sullivan, A. E., Hallber, G. R. & Horton, D. G. Vegetational changes in Western Illinois during the onset of Late Wisconsinan glaciation. *Ecology* **70**, 1363–1376 (1989).
43. Magyari, E., Jakab, G., Rudner, E. & Sümegi, P. Palynological and plant macrofossil data on Late Pleistocene short-term climatic oscillations in North-Eastern Hungary. *Acta Palaeobot.* **2** (Suppl.), 491–502 (1999).
44. Heusser, C. J. Palynology and phytogeographical significance of a late-Pleistocene refugium near Kalaloch, Washington. *Quat. Res.* **2**, 189–201 (1972).
45. Baker, R. G. et al. A full-glacial biota from southeastern Iowa, USA. *J. Quat. Sci.* **1**, 91–107 (1986).
46. Baker, R. G., Bettis, E. A. I. & Horton, D. G. Late Wisconsinan-early Holocene riparian paleoenvironment in southeastern Iowa. *Geol. Soc. Am. Bull.* **105**, 206–212 (1993).
47. Elias, S. A., Short, S. K., Nelson, C. H. & Birks, H. H. Life and times of the Bering land bridge. *Nature* **382**, 60–63 (1996).
48. Lowery, D., Wah, J. & Rick, T. Post-Last Glacial Maximum dune sequence for the 'Parsonburg' Formation at Elliot's Island, Maryland. *Curr. Res. Pleistocene* **28**, 103–104 (2011).
49. Zhao, Y. et al. Peatland initiation and carbon accumulation in China over the last 50,000 years. *Earth Sci. Rev.* **128**, 139–146 (2014).
50. Andreev, A. A. et al. Late Pleistocene and Holocene vegetation and climate on the Taymyr Lowland, northern Siberia. *Quat. Res.* **57**, 138–150 (2002).
51. Paus, A., Svendsen, J. I. & Matiouchkov, A. Late Weichselian (Valdaian) and Holocene vegetation and environmental history of the northern Timan Ridge, European Arctic Russia. *Quat. Sci. Rev.* **22**, 2285–2302 (2003).
52. de Beaulieu, J.-L. & Reille, M. A long Upper Pleistocene pollen record from Les Echets, near Lyon, France. *Boreas* **13**, 111–132 (1984).
53. Magyari, E. K. et al. Vegetation and environmental responses to climate forcing during the Last Glacial Maximum and deglaciation in the East Carpathians: attenuated response to maximum cooling and increased biomass burning. *Quat. Sci. Rev.* **106**, 278–298 (2014).
54. Bos, J. A. A., Bohncke, S. J. P., Kasse, C. & Vandenberghe, J. Vegetation and climate during the Weichselian early glacial and pleniglacial in the Niederlausitz, eastern Germany—macrofossil and pollen evidence. *J. Quat. Sci.* **16**, 269–289 (2001).
55. Müller, S. et al. Late Quaternary vegetation and environments in the Verkhoyansk Mountains region (NE Asia) reconstructed from a 50-kyr fossil pollen record from Lake Billyakh. *Quat. Sci. Rev.* **29**, 2071–2086 (2010).
56. Demske, D. et al. Late glacial and Holocene vegetation and regional climate variability evidenced in high-resolution pollen records from Lake Baikal. *Global Planet. Change* **46**, 255–279 (2005).
57. Igarashi, Y. & Zharov, A. E. Climate and vegetation change during the late Pleistocene and early Holocene in Sakhalin and Hokkaido, northeast Asia. *Quat. Int.* **237**, 24–31 (2011).
58. Svendsen, J. I. et al. Glacial and vegetation history of the Polar Ural Mountains in northern Russia during the Last Ice Age, Marine Isotope Stages 5-2. *Quat. Sci. Rev.* **92**, 409–428 (2014).
59. Zech, M. et al. Quaternary vegetation changes derived from a loess-like permafrost palaeosol sequence in northeast Siberia using alkane biomarker and pollen analyses. *Boreas* **39**, 540–550 (2010).
60. Wetterich, S. et al. Last Glacial Maximum records in permafrost of the East Siberian Arctic. *Quat. Sci. Rev.* **30**, 3139–3151 (2011).
61. Wetterich, S. et al. Palaeoenvironmental dynamics inferred from late Quaternary permafrost deposits on Kurungnakh Island, Lena Delta, Northeast Siberia, Russia. *Quat. Sci. Rev.* **27**, 1523–1540 (2008).
62. Shichi, K. et al. Vegetation response in the southern Lake Baikal region to abrupt climate events over the past 33 cal kyr. *Palaeogeogr. Palaeoclimatol. Palaeoecol.* **375**, 70–82 (2013).
63. Bolikhovskaya, N. S. & Shunkov, M. V. Pleistocene environments of Northwestern Altai: vegetation and climate. *Archaeol. Ethnol. Anthropol. Eurasia* **42**, 2–17 (2014).
64. Neotoma Paleoecology Database. Neotoma https://www.neotomadb.org/ (2016).
65. Grieser, J., Gommes, R., Cofield, S. & Barandi, M. Data sources for FAO worldmaps of Koeppen climatologies and climatic net primary production. *Food and Agriculture Organization of the United Nations* http://www.fao.org/nr/climpag/globgrids/KC_commondata_en.asp (2006).
66. Gorczynski, W. Sur le calcul du degré de continentalisme et son application dans la climatologie. *Geogr. Ann.* **2**, 324–331 (1920).
67. Scheff, J., Seager, R., Liu, H. & Coats, S. Are glacials dry? Consequences for paleoclimatology and for greenhouse warming. *J. Clim.* **30**, 6593–6609 (2017).
68. Bartlein, P. J. et al. Pollen-based continental climate reconstructions at 6 and 21 ka: a global synthesis. *Clim. Dyn.* **37**, 775–802 (2011).
69. Brown, J., Ferrains, O., Heginbottom, J. & Melnikov, E. Circum-Arctic map of permafrost and ground-ice conditions, version 2. *National Snow and Ice Data Center* https://nsidc.org/data/ggd318 (2002).
70. Hugelius, G. et al. A new data set for estimating organic carbon storage to 3 m depth in soils of the northern circumpolar permafrost region. *Earth Syst. Sci. Data* **5**, 393–402 (2013).
71. Batjes, N. H. Harmonized soil property values for broad-scale modelling (WISE30sec) with estimates of global soil carbon stocks. *Geoderma* **269**, 61–68 (2016).
72. Jobbágy, E. G. & Jackson, R. B. The vertical distribution of soil organic carbon and its relation to climate and vegetation. *Ecol. Appl.* **10**, 423–436 (2000).
73. Gorham, E. Northern peatlands: role in the carbon cycle and probable responses to climatic warming. *Ecol. Appl.* **1**, 182–195 (1991).
74. Lehner, B. & Döll, P. Development and validation of a global database of lakes, reservoirs and wetlands. *J. Hydrol. (Amst.)* **296**, 1–22 (2004).
75. Amosov, M. Lake-levels, vegetation and climate in Central Asia during the Last Glacial Maximum. *Russ. Geogr. Soc. Her.* (in Russian) **910–911**, 1–14 (2014).
76. Ebel, T., Melles, M. & Niessen, F. in *Land-Ocean Systems in the Siberian Arctic: Dynamics and History* (eds. Kassens, H. et al.) 425–435 (Springer-Verlag, 1999).
77. Colman, S. M., Carter, S. J., Hatton, J. & Haskell, B. J. *Cores collected in Lake Baikal, Siberia, by the U.S. Geological Survey, 1990 to 1992: Visual Descriptions, Photographs, X-radiographs, Bulk-Density Measurements, and Grain-Size Analyses* (US Dept Interior Geol. Surv. Open-File Report 94-445, 1992).
78. Orem, W. H., Colman, S. M. & Lerch, H. E. Lignin phenols in sediments of Lake Baikal, Siberia: application to paleoenvironmental studies. *Org. Geochem.* **27**, 153–172 (1997).
79. Teller, J. T. & Last, W. M. Late Quaternary History of Lake Manitoba, Canada. *Quat. Int.* **16**, 97–116 (1981).
80. Lim, J., Woodward, J., Tulaczyk, S., Christoffersen, P. & Cummings, S. P. Analysis of the microbial community and geochemistry of a sediment core from Great Slave Lake, Canada. *Antonie van Leeuwenhoek* **99**, 423–430 (2011).
81. Ruesch, A. & Gibbs, H. K. New IPCC Tier-1 Global Biomass Carbon Map for the Year 2000. *Carbon Dioxide Information Analysis Center* http://cdiac.ess-dive.lbl.gov (2008).
82. Ehlers, J., Gibbard, P. & Hughes, P. *Quaternary Glaciations—Extent and Chronology: A Closer Look* (Elsevier, London, 2011).
83. Clark, P. U. et al. The Last Glacial Maximum. *Science* **325**, 710–714 (2009).
84. Amante, C. & Eakins, B. W. *ETOPO1 1 Arc-Minute Global Relief Model: Procedures, Data Sources and Analysis* (NOAA Technical Memorandum NESDIS-NGDC-24, Boulder, Colorado, 2009).
85. Siewert, M. B., Hugelius, G., Heim, B. & Faucherre, S. Landscape controls and vertical variability of soil organic carbon storage in permafrost-affected soils of the Lena River Delta. *Catena* **147**, 725–741 (2016).
86. Lewis, G., Fosberg, M., McDole, R. & Chugg, J. Distribution and some properties of loess in south-central and south-eastern Idaho. *Soil Sci. Soc. Am. Proc.* **39**, 1165–1168 (1975).
87. Romanovsky, N. N. *Fundamentals of Cryogenics of Lithosphere* (Moscow Univ. Press, Moscow, 1993).
88. Busacca, A. & McDonald, E. Regional sedimentation of late Quaternary loess on the Columbia Plateau: sediment source areas and loess distribution patterns, regional geology of Washington State. *Washingt. Div. Geol. Earth Resour. Bull.* **80**, 181–190 (1994).
89. Bettis, E. A., Muhs, D. R., Roberts, H. M. & Wintle, A. G. Last Glacial loess in the conterminous USA. *Quat. Sci. Rev.* **22**, 1907–1946 (2003).
90. Haase, D. et al. Loess in Europe-its spatial distribution based on a European Loess Map, scale 1:2,500,000. *Quat. Sci. Rev.* **26**, 1301–1312 (2007).
91. Muhs, D. R. The geologic records of dust in the quaternary. *Aeolian Res.* **9**, 3–48 (2013).

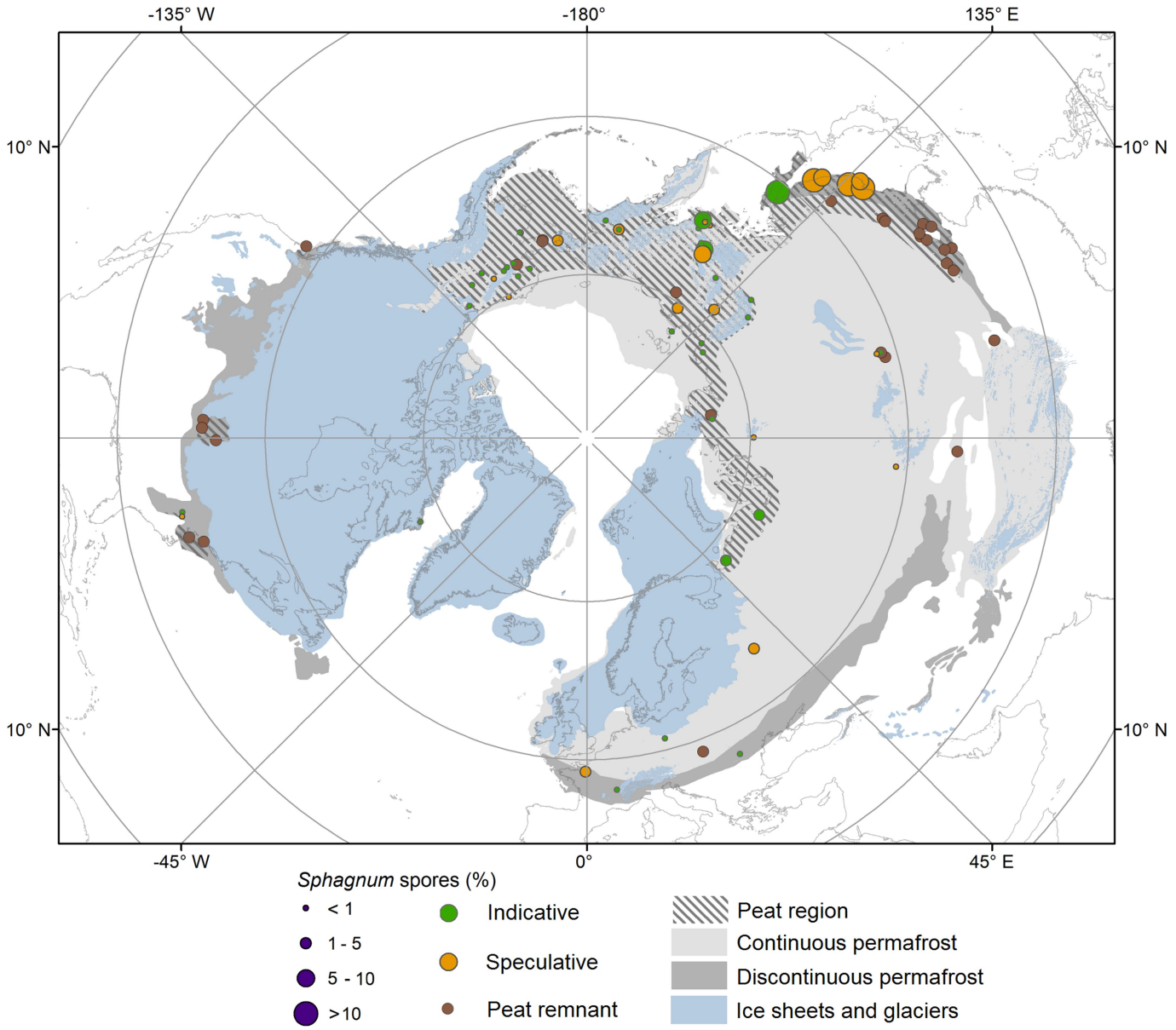

Extended Data Fig. 1 | LGM peat region. The reconstructed peat region is based on already-reconstructed areas[40,41], *Sphagnum* spore evidence, and the occurrence of peat[42,43] or peaty layers[44–49]. The colouring and size of these points show the percentage of the total pollen sum that was spores (not algae) and our interpretation of the reliability of the dating. Indicative ages are better constrained than speculative ages (see Supplementary Information). Evidence of dated peat or peaty deposits is shown in dark brown. Data for ice sheets and glaciers are modified from ref. [82], and the permafrost region[11] is included for reference.

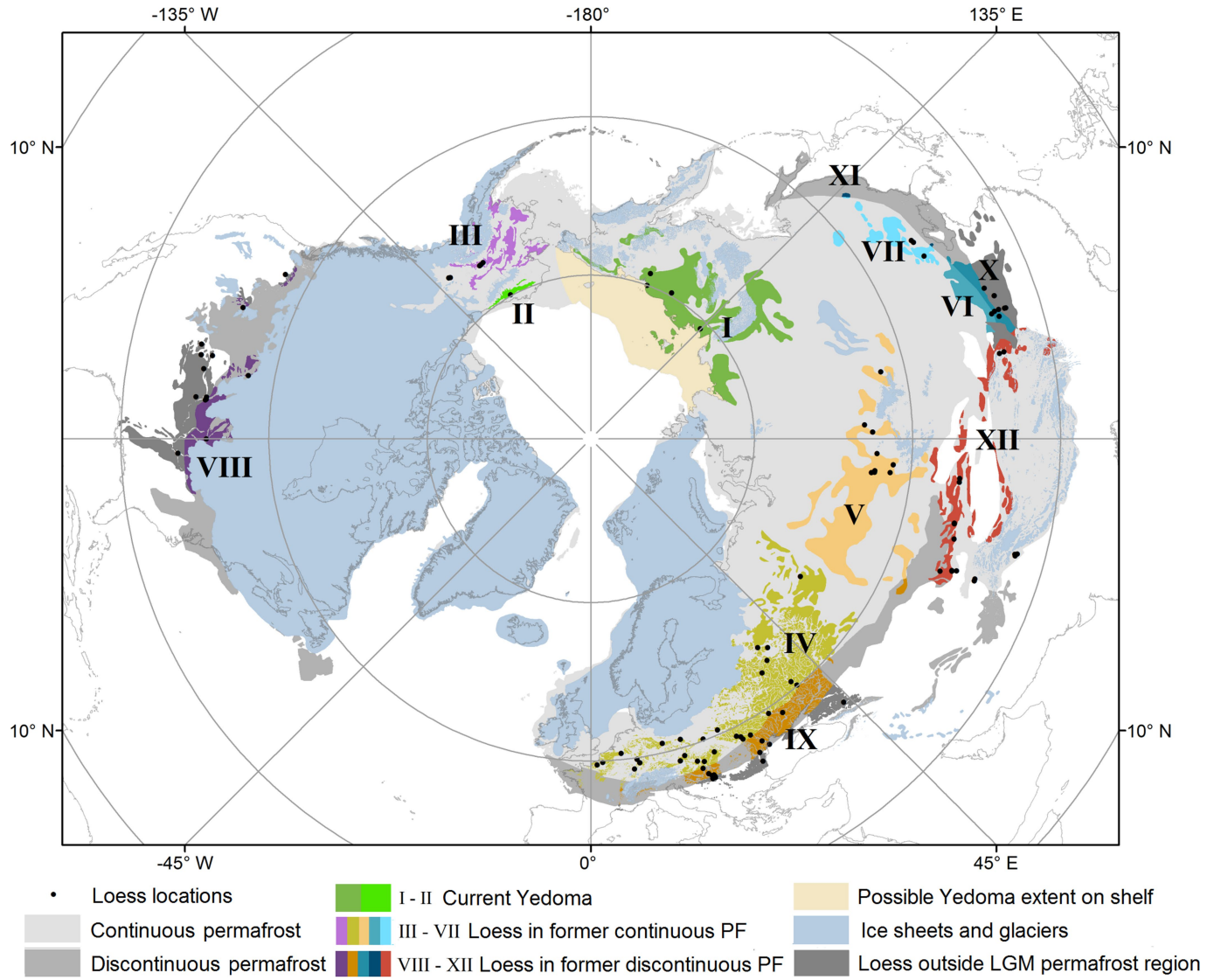

Extended Data Fig. 2 | Loess and Yedoma deposits during the LGM. The deposits were compiled from several data sources[86–91], and separated into sections (shown with Latin numerals) as described in Methods and Supplementary Information. The loess extent outside of the LGM continuous permafrost region is included for reference[89]. A tentative area of Yedoma extent on the shelf is also included. We assume that this area had the same degree of dissection as the Yedoma on land (see Supplementary Information). Data for ice sheets and glaciers are modified from ref. [82], and the permafrost region[11] is included for reference. PF, permafrost.

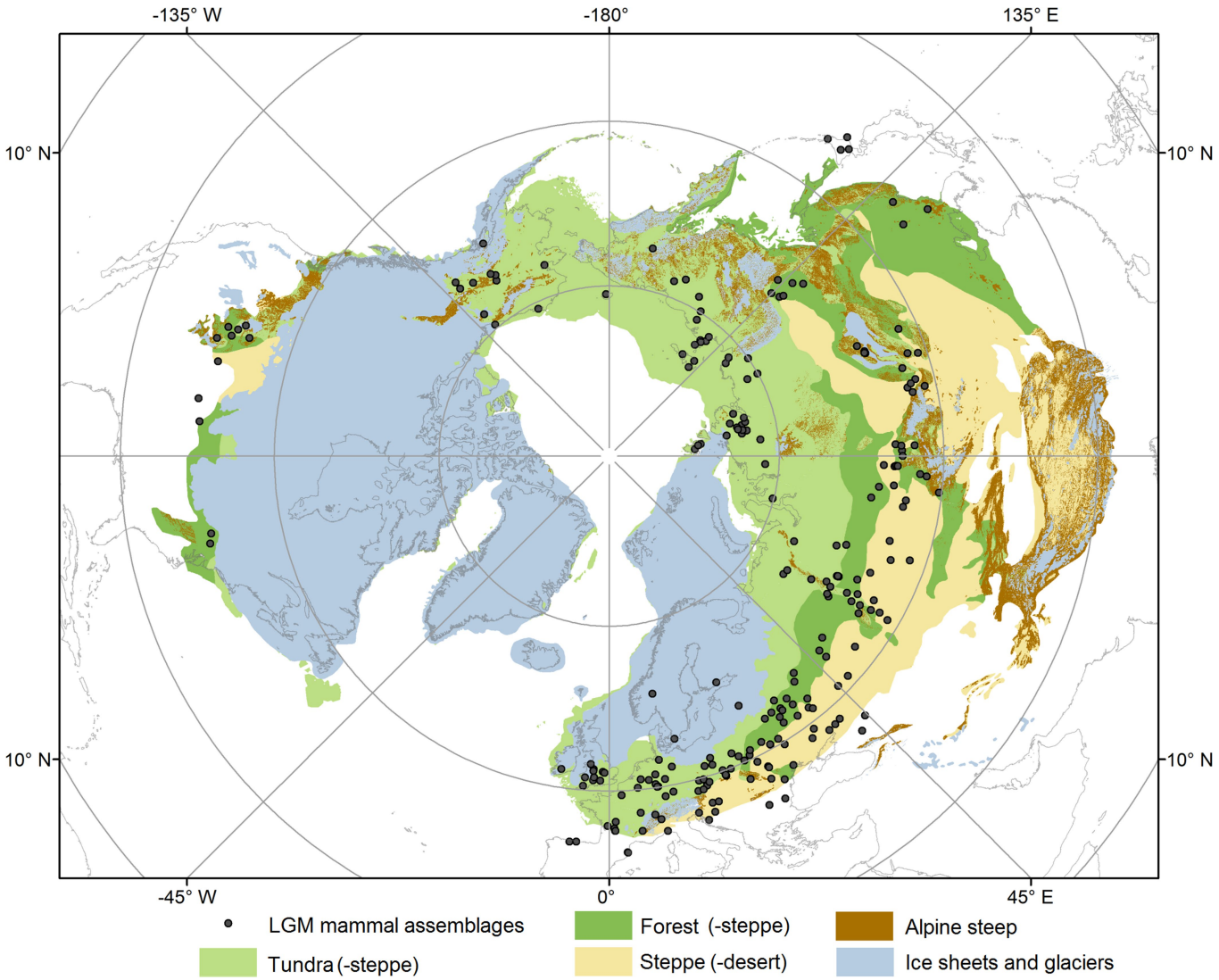

Extended Data Fig. 3 | LGM mega biomes and LGM mammal assemblages. Assemblages of mammoths, horses, bison, reindeer, wholly rhinoceroses and muskoxen[17,31,32] dated to between 18 kyr BP and 26 kyr BP indicate an environment that was productive enough to support megafauna (see Supplementary Information). Note that none of the data points within the Fennoscandian Ice Sheet are younger than 19 kyr BP. Data for ice sheets and glaciers are modified from ref. [82].

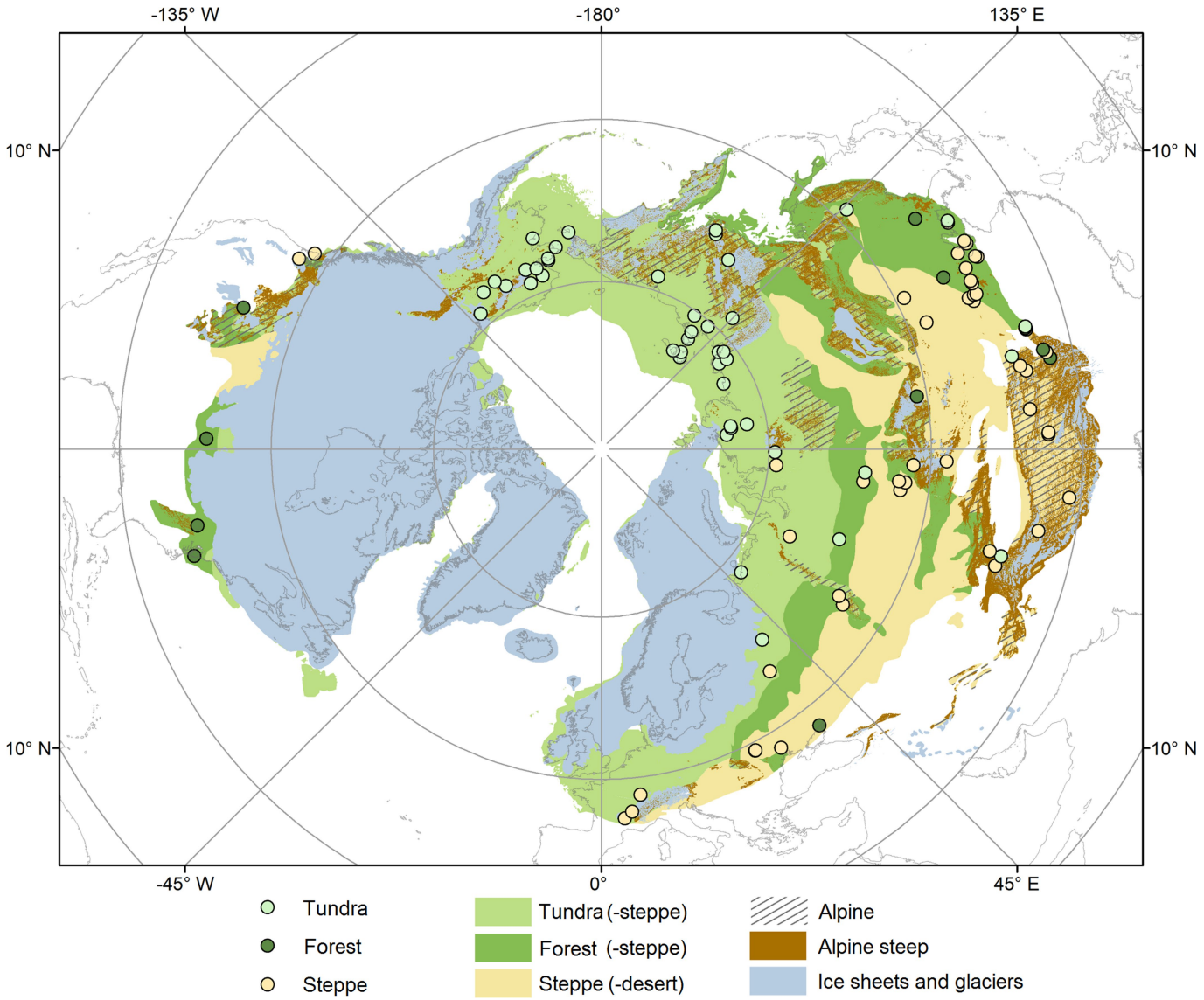

Extended Data Fig. 4 | The LGM mega biomes, and point data from pollen and macrofossil findings. The map shows the major biomes within the LGM permafrost region, constructed from three separate empirical maps[15–17], as well as our additional separation of alpine environments and steep areas[18]. Biomized pollen data and macrofossil findings[9,33–36] were compared with the reconstruction to assess its accuracy (see Supplementary Information). Data for ice sheets and glaciers are modified from ref. [82].

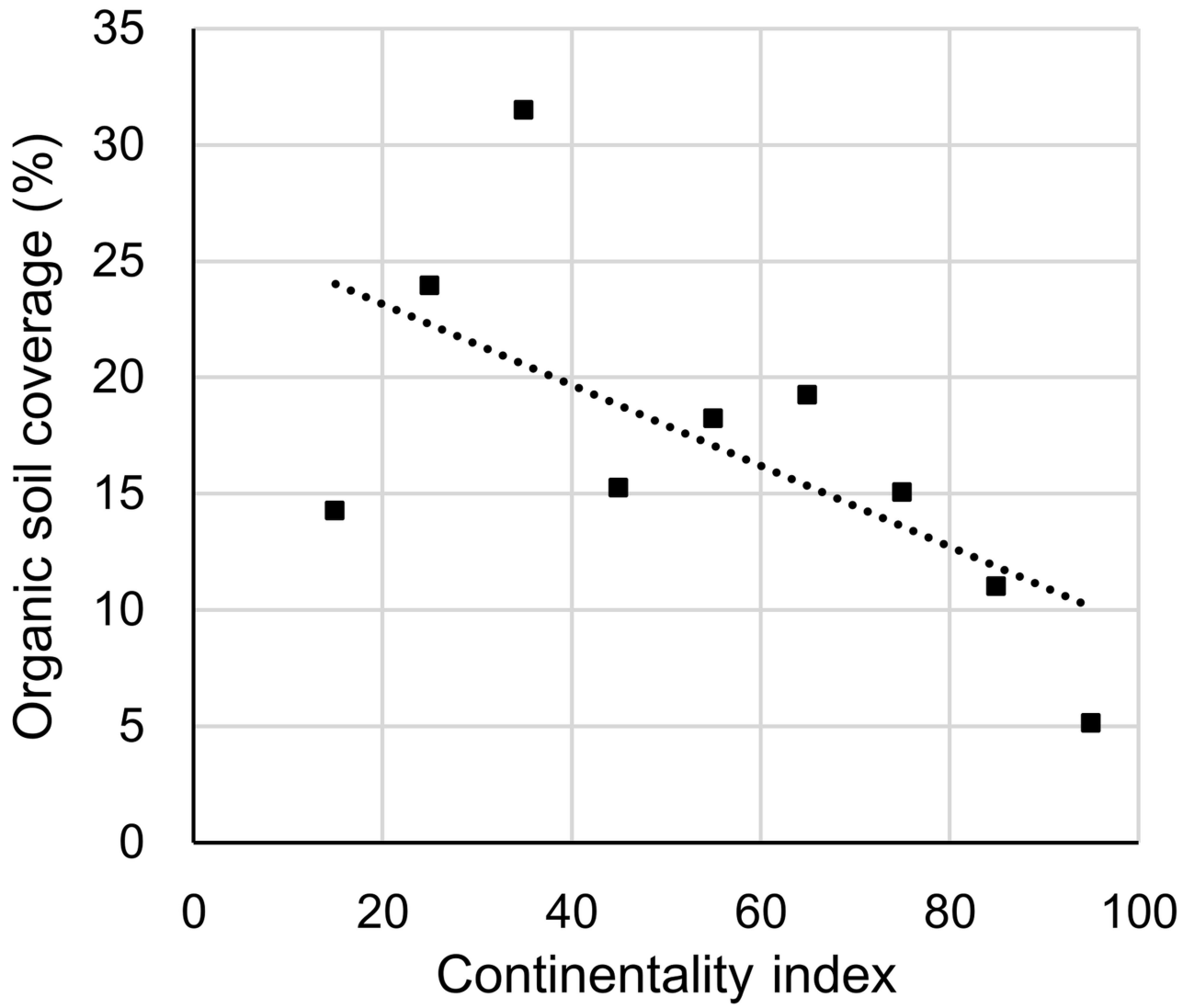

Extended Data Fig. 5 | Regression between continentality and organic soil coverage. The organic soil (peat) coverage was calculated from data within the NCSCDv2 database for flat terrain only (see Supplementary Information). The data were aggregated into classes of continentality, determined from the map[65] of the Gorczynski continentality index[66] (see Methods). The trend indicates that peat coverage in flat terrain is lower in regions with high continentality ($R^2 = 0.4$) than in regions of low continentality.

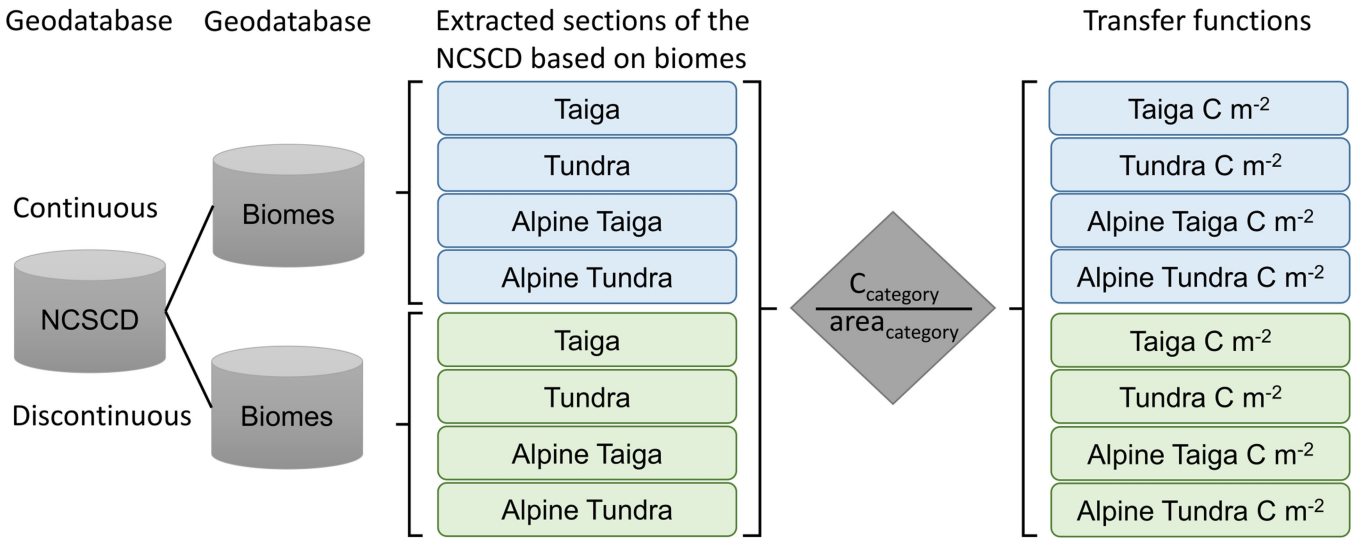

Extended Data Fig. 6 | A schematic presentation of data handling for soil of depth 0–1 m. To estimate LGM soil carbon, we used databases to calculate carbon-transfer functions for different biomes. The colouring describes the continuous and discontinuous sections that were separated before applying the biomes as a second filter. Modern-day biomes were overlain with modern-day carbon stocks in permafrost terrain, providing biome-specific information that was translated into transfer functions (see Methods).

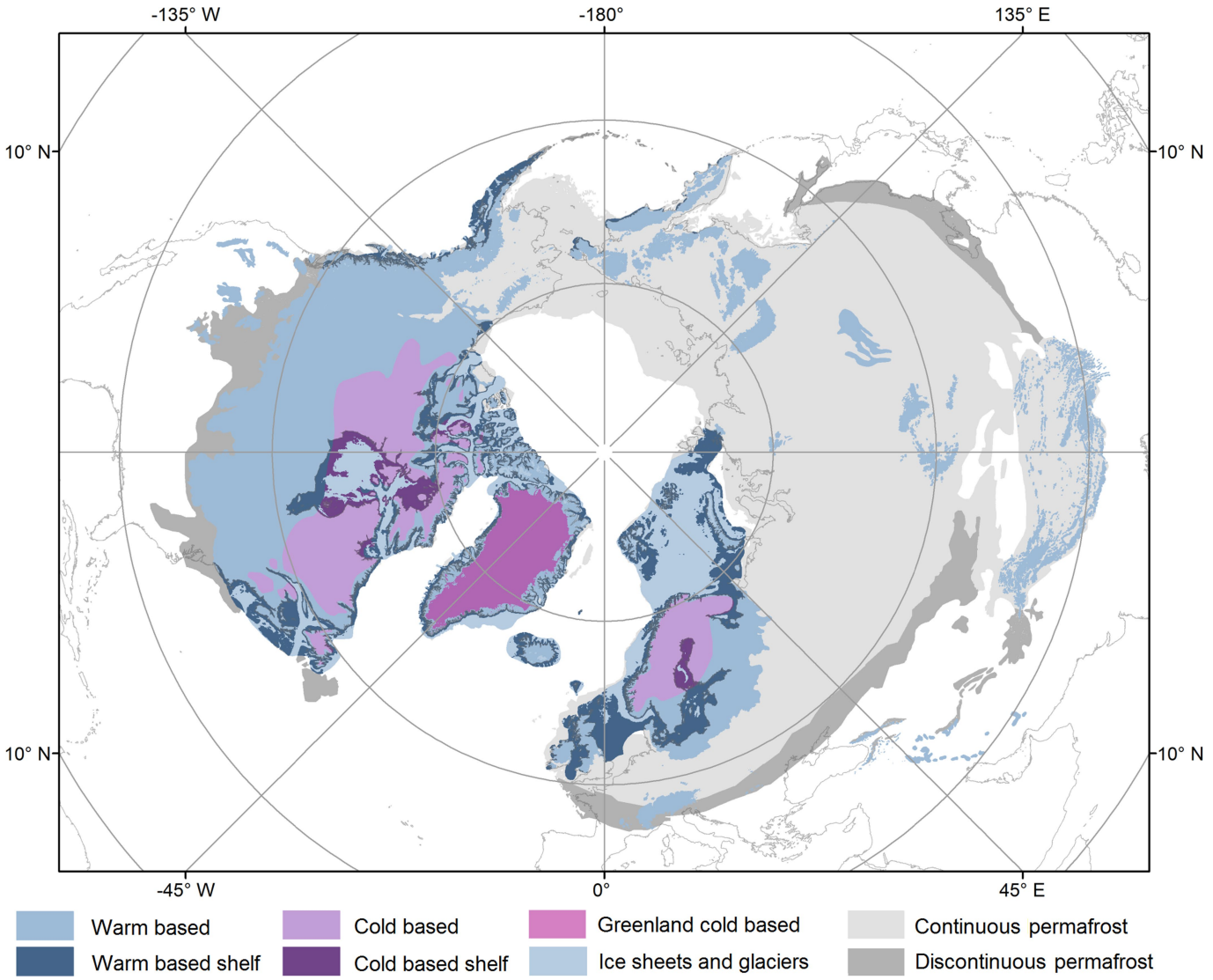

Extended Data Fig. 7 | Warm-based and cold-based sections of ice sheets and glaciers[24,69], both on land and on shelves. Cold-based areas are assumed to retain the carbon storage formed before the glaciation. Warm-based ice sheets and glaciers, on the other hand, are erosive, and we assume no preserved carbon storage. Data for ice sheets and glaciers are modified from ref. [82], and the permafrost region[11] is included for reference.

Extended Data Table 1 | Biome categories included under each 'mega' biome for lowland and alpine areas

Lowland		
Tundra (-steppe)	**Forest (-steppe)**	**Steppe (-desert)**
Tundra	Coniferous/broad-leaved and montane forest	Mammoth tundra steppe (boreal)
Complex of tundra steppe forest, local halophytic	Open pine forest of low-mountainous regions	Grass steppe and scattered flatland semi desert
Mammoth tundra steppe (arctic)	Appalachian forest	Periglacial steppe dominated by European elements
Subarctic desert, montane tundra, subalpine meadows[1]	Boreal forest	Periglacial steppe dominated by Mongolian elements
	Floridan forest subtropical	Mixed-grass flatland steppe
	Forest tundra	Mongolian desert steppe
	Dark coniferous and birch montane forest	Montane steppe and semi desert
	Forest refugia	Central North American steppe
	Forest steppe with birch and pine	Mixed mammoth tundra-steppe (boreal) w. steppe
	Japan-Chinese forest steppe	Steppe
	Light coniferous montane forest	Pontian-Kazakhstan steppe
	Mixed mammoth tundra-steppe (boreal) w. forest steppe	
	Open birch and spruce forest	
	Open forest – larch and birch with tundra elements	
	Periglacial forest steppe, larch pine birch tundra	
	Subalpine forest*	
	Mixed mammoth tundra steppe (boreal) w. forest	
	Forest steppe with European broadleaf trees	
Alpine		
Tundra (-steppe)	**Forest (-steppe)**	**Steppe (-desert)**
Subarctic desert, montane tundra, subalpine meadows	Subalpine forest	Mountain desert
Alpine tundra		Montane steppe and semi desert

*Classified as lowland on shelf areas.

Extended Data Table 2 | Areas, carbon-transfer functions and carbon stocks (in Pg C) at the LGM

Environment	Permafrost	Area km^2	30 cm kg Cm^{-2}	0 - 1m kg Cm^{-2}	1 - 2 m kg Cm^{-2}	2 -3 m kg Cm^{-2}	Pg C
Lowland*							
Steppe (-desert)	continuous	6,424,000	4.2	7.5	3.1	2.8	86
	discontinuous	1,813,000	4.2	7.5	3.1	2.8	24
Forest (-steppe)	continuous	5,085,000	9.4	20.2	10.1	12.1	217
	discontinuous	1,413,000	8.4	14.8	7.4	8.9	45
Tundra (-steppe)	continuous	10,353,000	11.2	26.7	12.8	10.8	527
	discontinuous	635,000	9.2	13.1	6.3	5.3	16
Peat	continuous	416,000	16.9	63.1	-	-	26
	discontinuous	76,000	17.5	62.2	-	-	5
Alpine							
steep >4 deg	N/A	4,084,000	-	3.0	-	-	12
Steppe (-desert)	continuous	1,288,000	4.2	7.5	3.1	2.8	17
	discontinuous	198,000	4.2	7.5	3.1	2.8	3
Forest (-steppe)	continuous	12,000	10.1	13.5	6.7	8.1	0.3
	discontinuous	187,000	5.5	11.7	5.8	7.0	5
Tundra (-steppe)	continuous	2,147,000	5.2	11.4	5.5	4.6	47
	discontinuous	201,000	6.6	13.6	6.5	5.5	5
Peat	continuous	74,000	19.4	67.2	-	-	5
	discontinuous	8,000	14.7	69.4	-	-	1
Glacial burial							
Cold based		4,320,000	-	17.8	6.9	2.8	119
Cold based peat		44,000	-	63.1	-	-	3
Cold based steep		304,000	-	3.0	-	-	1
Greenland		1,713,000		17.8	6.9	2.8	47
Greenland peat		17,000	16.9	63.1	-	-	1
Deep deposits							
Yedoma		1,200,000					301
Loess		2,700,000					366
Yedoma on shelf		1,600,000					349
Delta		76,000					91
Lakes							
Large Lakes		70,000					2

*Shelf areas and resulting carbon stocks are included under the lowland category.

Extended Data Table 3 | Estimates of areas and carbon stocks (in Pg C) beneath ice sheets and glaciers

Environment	Area	0 - 1 m C m^{-2}	1 - 2 m C m^{-2}	2- 3 m C m^{-2}	Pg C
		Land			
Cold based	3,773,000	17.8	6.9	2.8	104
Cold based peat	38,000	63.1			2.4
Alpine steep	304,000	3.0			0.9
Warm based (not Greenland)	9,789,000	*17.8*	6.9	2.8	*270*
Warm based peat	99,000	*63.1*			*6.2*
Alpine steep	2,675,000	*3.0*			*8.0*
		Shelf			
Cold based	547,000	17.8	6.9	2.8	15
Cold based peat	6,000	63.1			0.3
Alpine steep	0	3.0			0.0
Warm based (not Greenland)	2,821,000	*17.8*	6.9	2.8	*77.8*
Warm based peat	28,000	*63.1*			*1.8*
Alpine steep	0	*3.0*			

RESEARCH LETTER

Author Queries

Journal: **Nature**
Paper: **s41586-018-0371-0**
Title: **Extensive loss of past permafrost carbon but a net accumulation into present-day soils**

AUTHOR:

The following queries have arisen during the editing of your manuscript. Please answer by making the requisite corrections directly in the e.proofing tool rather than marking them up on the PDF. This will ensure that your corrections are incorporated accurately and that your paper is published as quickly as possible.

Query Reference	Query
Q1	This proof has been produced on the basis of your corrections to the preproof. For this later stage of production we use an online 'eproof' tool, in which you can make corrections to the text directly and mark up corrections to the copyedited figures. You will receive a link to the eproof tool via email later in the production process. When you receive the eproof link, please check that the display items are as follows (ms no: 2017-08-11646): Figs 2 (colour); Tables, 1; Boxes, none; Extended Data display items, 7 Figs, 3 Tables; SI, yes. The eproof contains the main-text figures edited by us and (if present) the Extended Data items (unedited except for the legends) and the Supplementary Information (unedited). Please note that the eproof should be amended in only one browser window at any one time, otherwise changes will be overwritten. Please check the edits to all main-text figures (and tables, if any) very carefully, and ensure that any error bars in the figures are defined in the figure legends. Extended Data items may be revised only if there are errors in the original submissions. If you need to revise any Extended Data items please upload these files when you submit your corrections to this preproof.
Q2	Author surnames have been highlighted - please check these carefully and indicate if the first name or surname have been marked up incorrectly. Please note that this will affect indexing of your article, such as in PubMed.
Q3	[Authors: please check this legend carefully]